

---

# SHIELD: A Diverse Clinical Note Dataset and Distilled Small Language Models for Enterprise-Scale De-identification

---

**Jose D. Posada\***  
Technology & Digital Solutions  
Stanford Medicine

**David Love**  
Technology & Digital Solutions  
Stanford Medicine

**Somalee Datta**  
Technology & Digital Solutions  
Stanford Medicine

**Priya Desai**  
Technology & Digital Solutions  
Stanford Medicine

## Abstract

De-identification of clinical text remains a critical prerequisite for the secondary use of electronic health records (EHRs). Existing public benchmarks, notably the i2b2 2006 and 2014 corpora, are over a decade old and lack the semantic and demographic diversity of modern clinical narratives. Furthermore, while Large Language Models (LLMs) demonstrate state-of-the-art zero-shot extraction capabilities, their use at enterprise scale is hindered by massive computational costs and strict hospital data governance that restricts sending Protected Health Information (PHI) to cloud APIs. We introduce SHIELD (Synthetic Human-annotated Identifier-replaced Entries for Learning and De-identification), a diverse clinical note dataset containing 1,394 notes with 10,505 gold-standard PHI spans across 9 categories, built using set-cover diversity sampling across demographic and document-type strata with human-in-the-loop adjudication. We evaluate four LLMs—two proprietary and two open-weight—establishing a performance ceiling on SHIELD, then demonstrate that a teacher-student distillation framework transfers these capabilities into locally deployable Small Language Models (SLMs). Distributional divergence analysis (Fréchet Text Distance and Jensen–Shannon Divergence) demonstrates that SHIELD occupies a distinct region of biomedical embedding and vocabulary space compared to legacy benchmarks. Our best distilled model closely matches its teacher on most structured PHI categories (DATE, DOCTOR, ID, PATIENT, PHONE) and achieves micro-averaged span-level precision of 0.88 and recall of 0.86, while running on standard workstation hardware. Cross-dataset evaluation across multiple corpora from different institutions shows that diversity-trained models generalize well on universal structured PHI categories, while institution-specific entities remain challenging to transfer in both directions—suggesting that optimal deployment may combine broad-coverage models with specialized models for high-volume, semi-structured note types. We publicly release the SHIELD dataset and the distilled DeBERTa v3 model to provide a high-accuracy, cost-effective de-identification pipeline deployable entirely behind institutional firewalls.

## 1 Introduction

**The data bottleneck in healthcare AI.** The digitization of medical records has created vast repositories of unstructured clinical text that are essential for data-driven medical research and

---

\*Corresponding author: [jdosada@stanford.edu](mailto:jdosada@stanford.edu)

the development of clinical artificial intelligence (AI) [Kather et al., 2024]. However, these free-text narratives are laden with Protected Health Information (PHI). Stringent privacy requirements mandated by regulations such as the Health Insurance Portability and Accountability Act (HIPAA) and the General Data Protection Regulation (GDPR) dictate that PHI must be thoroughly de-identified prior to secondary use or multi-institutional sharing. A recent systematic review of 69 studies confirmed that machine-learning and hybrid approaches now dominate clinical de-identification research, yet progress remains tightly coupled to the availability of high-quality annotated corpora [Kovačević et al., 2024]. Scoping reviews of the broader literature echo this finding, identifying annotated data scarcity as the primary bottleneck limiting deployment at scale [Negash et al., 2023].

**Limitations of existing approaches and benchmarks.** Historically, public benchmarks have driven methodological progress. The i2b2 2006 challenge provided the first shared evaluation for de-identification systems [Uzuner et al., 2007], and the i2b2 2014 corpus established a widely adopted standard [Stubbs and Uzuner, 2015]. Yet both datasets are now over a decade old, and have narrow focus on particular phenotypes. On the methods side, rule-based systems suffer from low precision and over-redaction; transformer-based models require costly local adaptation to each institution [Chambon et al., 2023]; and LLM-based approaches such as DeID-GPT [Liu et al., 2023] offer promising zero-shot capabilities but introduce hallucination risks, high inference costs, and data-governance concerns when PHI must traverse cloud APIs. Efforts to scale de-identification to billions of clinical notes [Kocaman et al., 2023] further underscore the need for systematic, multi-system evaluation frameworks [Heider and Meystre, 2024].

**Cross-institution generalization gap.** A critical but under-addressed challenge is the generalization gap: models trained on one institution’s corpus often fail when applied elsewhere. Yang et al. [2019] demonstrated that a deep-learning de-identification model’s F1 score dropped from 0.96 to 0.86 when evaluated across institutions. Recent studies at the US Department of Veterans Affairs [Eyre et al., 2025] and a multi-specialty UK hospital [Kuo et al., 2025] confirm that transformer transferability remains fragile, while real-world deployment experiences with AnonCAT [Kraljevic et al., 2023] highlight the operational difficulty of maintaining accuracy outside the training domain.

**Contributions.** To resolve these bottlenecks, we make four contributions:

- We introduce **SHIELD** (Synthetic Human-annotated Identifier-replaced Entries for Learning and De-identification), a new diverse benchmark with human-in-the-loop annotation using LLM pre-annotation and adjudication across 9 PHI categories.
- We present a knowledge-distillation framework that transfers the reasoning capabilities of a cloud LLM (Gemini 2.5 Flash) into Small Language Models (SLMs)—specifically DeBERTa v3 [He et al., 2021] and BioClinical ModernBERT [Sounack et al., 2025]—achieving near-teacher performance at a fraction of the cost, consistent with recent evidence that SLMs are poised to become the practical backbone of deployed AI systems [Belcak et al., 2025, Lee et al., 2025].
- We comprehensively evaluate four LLMs and four transformer models, establishing a performance ceiling on SHIELD and demonstrating cross-dataset generalization across three datasets (SHIELD, i2b2 2014, AIMI). We further quantify SHIELD’s distinctiveness through corpus divergence analysis—Fréchet Text Distance (FTD) and Jensen–Shannon Divergence (JSD)—showing that SHIELD is distributionally distinct from legacy benchmarks.
- We publicly release the SHIELD dataset and the distilled DeBERTa v3 model to lower the barrier to entry for clinical institutions wishing to safely unlock their EHR data.<sup>2</sup>

## 2 Methods

### 2.1 Dataset construction and diversity sampling

To construct a benchmark that genuinely reflects diverse patient populations and clinical scenarios, we bypassed traditional random sampling. Instead, we developed a sampling pipeline applied to the Stanford Medicine Research Data Repository, STARR-OMOP [Datta et al., 2020, Callahan

<sup>2</sup>Access instructions available at [https://github.com/susom/shield\\_dataset](https://github.com/susom/shield_dataset)

# SHIELD Annotation Pipeline

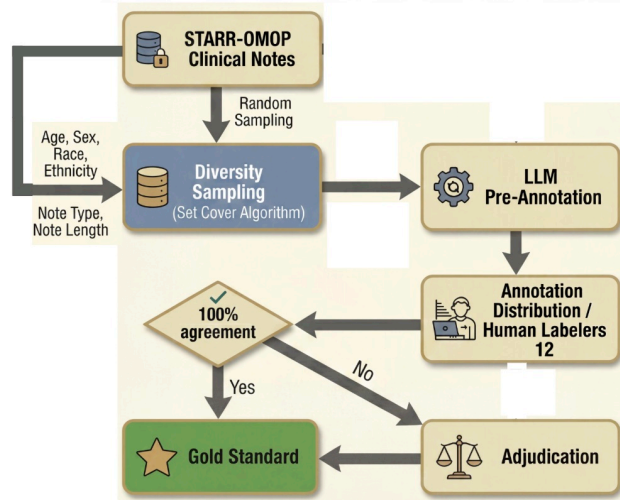


Figure 1: SHIELD annotation pipeline. Clinical notes are sampled from STARR-OMOP via diversity-optimized set cover, pre-annotated by an LLM, independently reviewed by two of 12 trained human labelers per note, and adjudicated to produce gold-standard PHI labels.

et al., 2023], containing over 158 billion tokens of clinical text. We utilized a Set Cover Algorithm [Williamson and Shmoys, 2011] optimized for diversity sampling across six demographic and document axes: age, sex, race, ethnicity, note type, and note length. This algorithm iteratively selects notes that maximize coverage of under-represented strata, producing a compact corpus that spans the full demographic landscape of the source warehouse.

The selected 1,394 notes underwent a rigorous human-in-the-loop annotation process (Figure 1). First, notes were pre-annotated using an LLM to identify candidate PHI spans. These pre-annotations were then distributed to a pool of 12 trained human labelers, with each note independently reviewed by two annotators. Spans achieving 100% inter-annotator agreement between the two reviewers were accepted directly into the gold standard; all disagreements underwent formal adjudication by a senior annotator. The final corpus contains 10,505 gold-standard PHI spans annotated across 9 PHI categories: AGE, DATE, DOCTOR, HOSPITAL, ID, LOCATION, PATIENT, PHONE, and WEB. To enable cross-dataset benchmarking against i2b2 2014 [Stubbs and Uzuner, 2015] and AIMI—a large-scale radiology report de-identification corpus developed by the AIMI Center at Stanford [Prakash et al., 2025], made available for this study through a research collaboration—all annotations were mapped into a unified canonical label taxonomy (see Appendix B for the complete mapping definitions).

## 2.2 Dataset release and surrogate replacement

The released SHIELD artifact is designed to protect patient privacy while preserving the linguistic structure required for meaningful evaluation of de-identification systems. Rather than redacting PHI spans, we replace each span with a type-appropriate cryptographic surrogate, yielding a corpus that reads as natural clinical text and supports end-to-end token- and span-level evaluation. A per-patient date jitter of 3–90 days is derived deterministically from each patient’s identifier via HMAC-SHA256 and applied uniformly to every date in that patient’s notes, preserving relative intervals between events while preventing calendar-based re-identification. Surrogates are generated by entity type: PATIENT and DOCTOR names are replaced using HIPS (Hash-based Identifier Pseudonymization System), DATE values receive the patient-specific jitter, ID and MRN values are replaced by irreversible keyed one-way hashes, PHONE and LOCATION values are mapped to format-preserving surrogates, and AGE is banded into ranges to prevent identification of extreme-age patients. Post-processing recomputes text hashes over the surrogate text, replaces patient identifiers with one-way hashes, and realigns each PHI span’s character offsets to the surrogate-replaced output. This approach follows the precedent established for the i2b2 2014 release [Stubbs and Uzuner, 2015] and recently applied

to MC-MED [Kansal et al., 2025]. Per-category PHI distribution, note-length statistics, patient demographics, and the most common note types are reported in Appendix G.

### 2.3 Corpus divergence analysis

To quantify how SHIELD differs from existing benchmarks (i2b2 2014 and AIMI), we applied two complementary distributional divergence metrics that together capture both semantic and lexical dimensions of corpus shift. Full mathematical formulations are provided in Appendix F.

**Fréchet Text Distance (FTD).** We measured distributional distance in biomedical embedding space using pre-computed 768-dimensional document embeddings from the MedCPT-Article-Encoder [Jin et al., 2023]. FTD—the text analog of Fréchet Inception Distance [Heusel et al., 2017], first applied to text evaluation as the Fréchet embedding distance by Moeed et al. [2020] and subsequently adopted for information retrieval evaluation by Arabzadeh and Clarke [2024]—computes the Fréchet distance [Dowson and Landau, 1982] between multivariate Gaussians fitted to each corpus’s embedding distribution, decomposed into a *mean shift* component (centroid displacement) and a *covariance divergence* component (differences in distributional spread and shape). Bootstrap 95% confidence intervals were computed via 1,000 subsampled resamples. Because bootstrap resampling with replacement reduces effective sample rank and systematically inflates the covariance divergence term of Fréchet-based distances [Chong and Forsyth, 2020], we report bootstrap mean estimates rather than full-data point estimates; this ensures that reported values fall within their corresponding CIs and provides a consistent set of estimates. The Fréchet distance is increasingly adopted across domains for corpus-level distributional comparison: in biomedical imaging, it remains the standard metric for evaluating generative models, though recent work cautions that domain-specific encoders are essential for meaningful scores [Wu et al., 2026]; in clinical retrieval-augmented generation, MedCPT embeddings serve as the backbone for systems such as RAD [Li et al., 2025], validating their suitability for capturing clinically relevant semantic structure. We chose MedCPT over general-purpose encoders because its contrastive pre-training on 255 million PubMed query–article pairs produces embeddings that prioritize clinical semantic similarity over surface-level lexical overlap [Jin et al., 2023].

**Jensen–Shannon Divergence (JSD).** We computed JSD [Lin, 1991] over whitespace-tokenized unigram frequency distributions to measure vocabulary-level divergence between corpus pairs. We report both equal-weight (standard) and corpus-size-weighted variants, with bootstrap mean estimates and 95% CIs via 1,000 document-level resamples. JSD is a well-established information-theoretic measure for corpus comparison, with recent applications ranging from optimizing client selection in federated learning to divergence-aware message-passing in graph neural networks [Wang and Yuan, 2025]. The choice of whitespace-tokenized unigrams—rather than subword tokens—is deliberate: recent work on vocabulary frequency imbalance shows that subword tokenizers increasingly skew token-frequency distributions as vocabulary size grows, which can mask genuine lexical differences between corpora [Chung and Kim, 2025]. By operating on raw unigrams, JSD captures the actual vocabulary divergence between clinical registers (e.g., physician jargon vs. patient colloquialisms) without artifacts introduced by tokenizer merge rules.

### 2.4 Model selection and distillation framework

Our objective was to bridge the gap between high-capability LLMs and firewall-friendly deployment. To establish a performance ceiling and select the best distillation teacher, we first evaluated four LLMs on the SHIELD gold standard in a zero-shot extraction setting. We tested two proprietary models—Gemini 2.5 Flash and Gemini 2.5 Flash Lite (Google)—and two open-weight models—OpenAI’s GPT-OSS 120B (117B total parameters, 5.1B active; Mixture-of-Experts) and GPT-OSS 20B (21B total, 3.6B active), both released under the Apache 2.0 license [OpenAI, 2025]. All LLMs were prompted with the same extraction template targeting the 9 canonical PHI categories (see Appendix D for the full prompt). This comparative evaluation directly informed teacher selection: the LLM with the strongest performance on high-risk PHI categories was chosen as the distillation teacher (Section 3.4).

We then constructed a three-stage teacher-student distillation pipeline (Figure 2):

1. **Prompt creation:** A small subset of the SHIELD gold standard was used solely to iteratively craft and refine extraction prompts. These prompts were validated against the gold standard

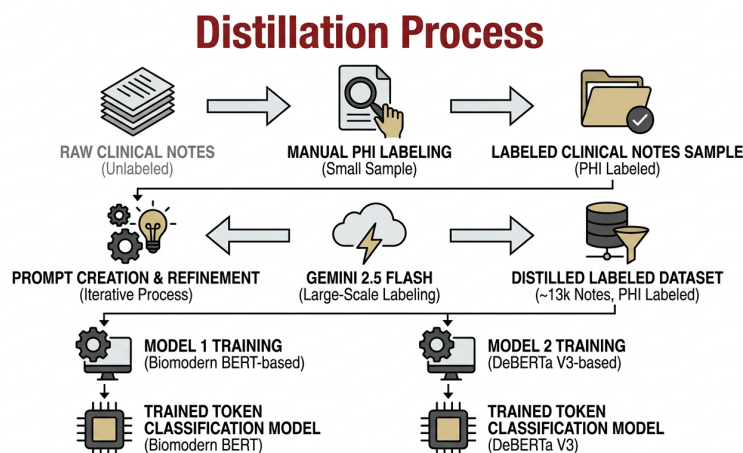


Figure 2: Teacher-student distillation process. A small labeled sample is used to create prompts for Gemini 2.5 Flash, which then labels  $\sim 13k$  notes. The distilled dataset trains DeBERTa v3 and BioClinical ModernBERT for local deployment.

until satisfactory precision and recall were achieved on the calibration set. Crucially, no SHIELD samples were used to train the student models.

2. **Large-scale teacher labeling:** The refined prompts were applied with Gemini 2.5 Flash to approximately 13,000 unlabeled clinical notes from the STARR-OMOP warehouse, generating silver-standard annotations at scale. Gemini 2.5 Flash was selected as the primary teacher due to its superior instruction-following, expansive context window, and state-of-the-art extraction accuracy.
3. **Student model training:** The distilled silver-standard labels were used to train two SLM architectures via token-level cross-entropy over BIO tags: DeBERTa v3 [He et al., 2021] and BioClinical ModernBERT [Sounack et al., 2025]. These two architectures were selected based on recent controlled comparisons showing that DeBERTa v3 offers superior sample efficiency and benchmark performance, while ModernBERT provides advantages in long-context support and inference speed [Antoun et al., 2025]. No SHIELD gold-standard annotations were included in the training data, preserving the entire SHIELD dataset as an independent evaluation set. These transformer architectures offer highly efficient inference, running on CPUs or consumer-grade edge GPUs within a hospital’s protected IT environment.

For comprehensive evaluation, we also benchmarked two prior-generation models—AIMI v1 and AIMI v2—developed by the AIMI Center at Stanford as part of their radiology report de-identification effort [Prakash et al., 2025]. Both models were trained on the AIMI dataset, a large-scale corpus of 46,313 radiology reports with gold-standard PHI annotations across 8 categories. The AIMI dataset is not publicly available; access was provided for this study through a collaboration with the AIMI researchers. AIMI v1 and v2 represent successive iterations of DeBERTa-based de-identification models trained on this domain-specific radiology data using the AIMI annotation pipeline. All four transformer models were evaluated on all three datasets (SHIELD, i2b2, AIMI) at both span-level and token-level granularity.

## 2.5 Statistical analysis

Span-level evaluation uses an overlap-based matching criterion: a predicted span is counted as a true positive if at least 80% of the gold span’s character length is covered by the prediction; unmatched predictions are false positives and unmatched gold spans are false negatives.

To quantify uncertainty in performance estimates—especially for low-support PHI categories—we computed bootstrap 95% confidence intervals (CIs) using document-level stratified resampling. For each evaluation, we resampled documents with replacement 2,000 times (seed = 42), recomputed span-level precision and recall per category on each bootstrap sample, and derived CIs using the percentile method. To test whether differences between models are statistically significant, we performed paired bootstrap tests: on each resample, the difference in recall between two models was computed, and the two-sided  $p$ -value was estimated as the proportion of bootstrap samples where the observed difference changed sign. All  $p$ -values were Bonferroni-corrected for multiple comparisons across the 9 PHI categories ( $\alpha = 0.05/9 \approx 0.0056$ ).

## 3 Results

### 3.1 SHIELD dataset statistics and semantic diversity

Figure 3(a) summarizes the three evaluation datasets. The final SHIELD dataset comprises 1,394 notes containing an estimated 406,294 tokens, 234,815 words, and 10,505 gold-standard PHI spans across 9 categories. While SHIELD is smaller in total note volume than AIMI (46,313 notes) its diversity sampling strategy was designed to capture a broad range of clinical language across demographic and document-type strata. Figure 3(b) shows the per-category PHI distribution across the three datasets.

Two complementary divergence analyses confirm that SHIELD is distributionally distinct from both i2b2 and AIMI.

**Embedding-space divergence (FTD).** Figure 4(a) presents the Fréchet Text Distance decomposition for all three corpus pairs. All pairs show  $FTD > 14$  with non-overlapping bootstrap 95% CIs, confirming statistically significant distributional separation in MedCPT embedding space. The FTD decomposition for SHIELD vs. i2b2 reveals substantial contributions from both mean shift (6.40) and covariance divergence (8.04), indicating that SHIELD differs from i2b2 in *both* centroid location and distributional shape—it is centered on genuinely different clinical content, not merely a wider version of i2b2 (which would show covariance-dominated FTD with minimal mean shift). The SHIELD–AIMI and i2b2–AIMI pairs show even larger FTD values (21.8 and 25.7, respectively), driven primarily by mean shift, reflecting AIMI’s radiology-specific content. Figure 4(b) visualizes the stacked decomposition.

**Vocabulary divergence (JSD).** Figure 4(c) presents the Jensen–Shannon Divergence for all three corpus pairs. The standard JSD between SHIELD and i2b2 (0.193) represents 28% of the theoretical maximum ( $\ln 2 \approx 0.693$ ), confirming measurably different token frequency distributions. The SHIELD–AIMI and i2b2–AIMI pairs show substantially higher standard JSD ( $\approx 0.47$ ), reflecting AIMI’s specialized radiology vocabulary. All bootstrap 95% CIs exclude zero.

### 3.2 LLM benchmark on SHIELD

Figure 5 presents the span-level performance of four LLMs evaluated on SHIELD in a zero-shot extraction setting (full numerical results in Table 1, Appendix A). All four models achieve strong performance across most PHI categories, confirming LLMs as viable de-identification tools. Gemini 2.5 Flash achieves the highest AGE recall (0.95) and HOSPITAL precision (0.85), motivating its selection as the distillation teacher. Flash Lite surprisingly excels on DATE ( $P = 0.99$ ,  $R = 0.95$ ) and PHONE ( $R = 0.95$ ), while the open-weight GPT-OSS models remain competitive but exhibit slightly lower recall on PATIENT and DOCTOR.

LOCATION is universally challenging: all LLMs achieve recall  $\leq 0.70$ , with Gemini Flash lowest at 0.59. WEB recall is also modest across the board (0.78–0.82) despite uniformly high precision ( $\geq 0.98$ ), as visualized in the radar profiles of Figure 5. These ceiling numbers set expectations for

(a)

Dataset	Notes	Tokens	Words	Vocab	PHI Spans
SHIELD	1,394	406,294	234,815	40,865	10,505
I2B2	1,304	1,399,589	805,117	73,091	28,867
AIMI	46,313	9,688,355	5,547,706	140,026	172,276

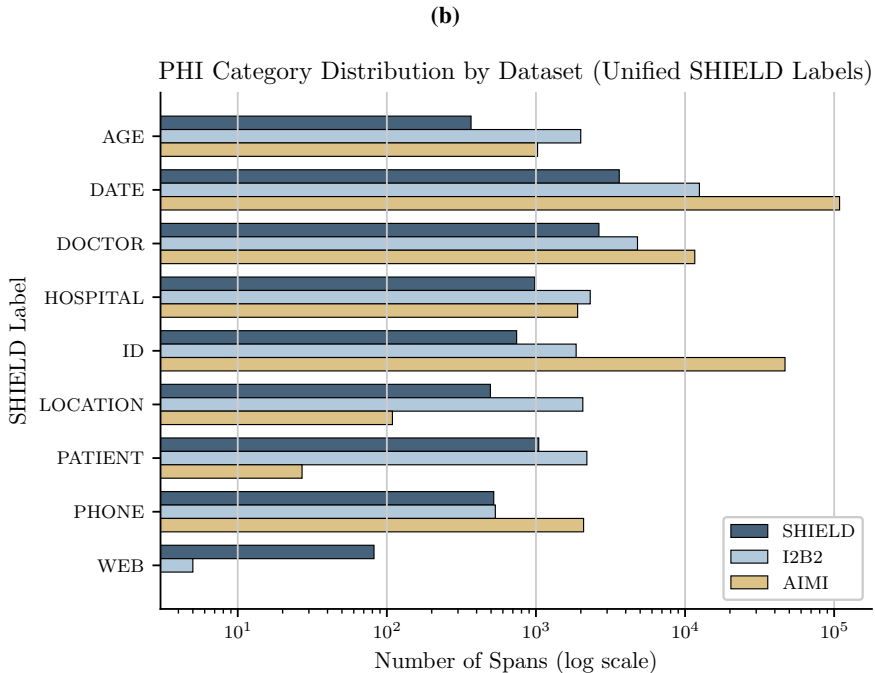


Figure 3: Dataset overview. (a) Statistics for the three evaluation corpora. (b) PHI category distribution across SHIELD, i2b2, and AIMI using the unified label taxonomy (log scale).

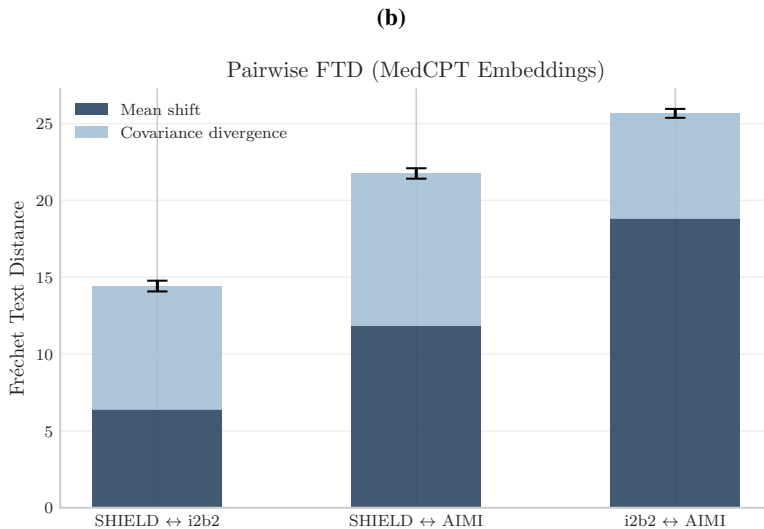
distillation: if the best LLM achieves recall of only 0.59 on LOCATION, the student model cannot be expected to surpass this limit.

### 3.3 Transformer model comparison on SHIELD

Having established the LLM performance ceiling in Figure 5, we now compare all four transformer models—two distilled students (DeBERTa v3 and BioClinical ModernBERT) and two non-student baselines (AIMI v1 and v2)—on the SHIELD gold standard. Figure 6 presents the span-level radar profiles, revealing that DeBERTa v3 is the best-performing student model and achieves the most uniform coverage across all 9 PHI categories. Among the two students, DeBERTa v3 achieves the highest point estimates on recall for DOCTOR (0.89 vs. 0.87), PATIENT (0.87 vs. 0.84), and HOSPITAL (0.74 vs. 0.69), though none of these differences reach statistical significance after Bonferroni correction. Compared with the non-student AIMI models, the students demonstrate a decisive advantage on categories absent from the AIMI training data: AIMI v1 scores 0.00 on AGE, LOCATION, and WEB, and AIMI v2 scores 0.00 on LOCATION and WEB, whereas DeBERTa v3 achieves recall of 0.77, 0.53, and 0.70 on these categories, respectively. On shared categories, the AIMI models achieve higher HOSPITAL recall (AIMI v1: 0.79 [0.76–0.82]) than the SHIELD-trained students (DeBERTa v3: 0.74 [0.70–0.77]), reflecting HOSPITAL as a domain-specific category, while DATE recall is statistically indistinguishable across all models (all within [0.92–0.93]). The full forest plot comparison with bootstrap CIs for both precision and recall across all three datasets appears in Figure 8.

(a)

Pair	FTD [95% CI]	Mean Shift [95% CI]	Cov. Divergence [95% CI]
SHIELD-i2b2	14.44 [14.08–14.78]	6.40 [6.15–6.64]	8.04 [7.88–8.23]
SHIELD-AIMI	21.76 [21.41–22.09]	11.83 [11.59–12.07]	9.93 [9.76–10.12]
i2b2-AIMI	25.67 [25.37–25.95]	18.81 [18.52–19.10]	6.86 [6.73–6.99]



(c)

Pair	JSD Standard [95% CI]	JSD Weighted [95% CI]
SHIELD-i2b2	0.193 [0.188–0.198]	0.145 [0.140–0.149]
SHIELD-AIMI	0.475 [0.470–0.480]	0.105 [0.103–0.107]
i2b2-AIMI	0.467 [0.464–0.470]	0.252 [0.247–0.256]

Figure 4: Corpus divergence analysis. (a) Fréchet Text Distance decomposed into mean shift and covariance divergence with bootstrap 95% CIs (1,000 resamples); reported values are bootstrap means. (b) Stacked FTD bar visualization; substantial contributions from both components for SHIELD-i2b2 indicate differences in both content focus and distributional shape. (c) Jensen-Shannon Divergence over unigram frequency distributions (standard and corpus-size-weighted variants); reported values are bootstrap means.

### 3.4 Distillation: SLMs matching LLMs

Given that DeBERTa v3 emerged as the strongest student in Figure 6, we examine in detail how well it reproduces its teacher’s capabilities. Gemini 2.5 Flash was selected as the distillation teacher based on its leading recall on high-risk categories (AGE: 0.95, PATIENT: 0.90) shown in Figure 5. Both student architectures were trained on the same ~13k distilled silver-standard samples; no SHIELD gold-standard annotations were used during training, preserving the entire SHIELD dataset as an independent held-out evaluation set. Figure 7 presents the teacher-vs.-student comparison for DeBERTa v3. The student closely matched the teacher on most span-level metrics, with significant degradation on two categories.

Paired bootstrap significance tests (Bonferroni-corrected,  $\alpha = 0.0056$ ; see Section 2.5) reveal two significant recall degradations from teacher to student: AGE ( $-0.17$ ,  $p = 0.005$ ) and HOSPITAL ( $-0.08$ ,  $p = 0.005$ ). No category shows a significant improvement. Differences on DATE ( $+0.02$ ,  $p = 0.855$ ), DOCTOR ( $+0.01$ ,  $p = 1.000$ ), ID ( $-0.03$ ,  $p = 1.000$ ), LOCATION ( $-0.06$ ,  $p = 1.000$ ), PATIENT ( $-0.03$ ,  $p = 0.190$ ), PHONE ( $+0.00$ ,  $p = 1.000$ ), and WEB ( $-0.11$ ,  $p = 0.585$ ) are not statistically significant after correction. These results confirm that DeBERTa v3 closely matches its teacher on most categories, with the remaining gaps concentrated in AGE and HOSPITAL (where the teacher’s generative reasoning may capture context that token-classification students miss) and

## LLM Comparison — SHIELD (Span-Level)

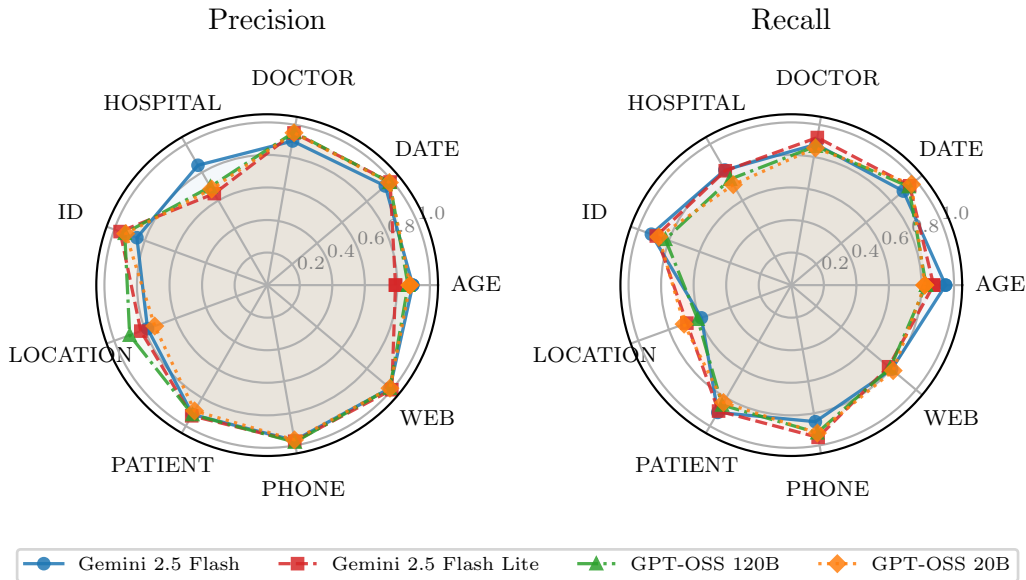


Figure 5: LLM benchmark on SHIELD. Span-level radar profiles showing precision (left) and recall (right) for four LLMs in zero-shot extraction. All models achieve strong coverage on structured categories (DATE, PHONE) but diverge on context-dependent entities (LOCATION, HOSPITAL). Full numerical results are provided in Table 1 (Appendix A).

low-support categories (WEB: 82 gold spans, 95% CI recall [0.55–0.85]; LOCATION: 495 gold spans, [0.48–0.59]) where bootstrap CIs are inherently wide.

### 3.5 Cross-dataset generalization

To assess whether SHIELD-trained models generalize beyond their training domain, we evaluated all four transformer models on i2b2 2014 and AIMI at span level. The forest plot in Figure 8 visualizes precision and recall with bootstrap 95% CIs across all three datasets simultaneously; full per-category numerical results are provided in Tables 4 and 5 (Appendix A), along with per-dataset radar profiles (Figures 9 and 10).

**Generalization to i2b2.** DeBERTa v3 leads on person-name categories: DOCTOR (0.85 [0.84–0.87]) and PATIENT (0.79 [0.77–0.82]), confirming that SHIELD-trained models generalize to i2b2’s clinical notes. AIMI v1/v2 achieve strong DATE recall (0.94 [0.93–0.95]) since dates are universal, but do not detect LOCATION (0.00), which was absent from their training data. All models score near zero on AGE due to label-definition differences between SHIELD and i2b2. HOSPITAL shows an interesting asymmetry: AIMI models achieve high recall (0.87 [0.85–0.88] for AIMI v1) with non-overlapping CIs against SHIELD-trained models (DeBERTa v3: 0.40 [0.37–0.42]), confirming that HOSPITAL recognition does not transfer across domains. These results are consistent with cross-institute generalization findings [Yang et al., 2019].

**Generalization to AIMI.** On AIMI’s home dataset, AIMI v2 achieves near-perfect recall on its core categories: DOCTOR 1.00 [1.00–1.00], ID 1.00 [1.00–1.00], and HOSPITAL 0.99 [0.99–1.00]. Only AIMI v2 detects AGE on AIMI (0.98 [0.97–0.99]); all other models score 0.00. DeBERTa v3 remains competitive on universal categories—DATE (0.94 [0.94–0.95]), ID (0.96 [0.95–0.96]), PHONE (0.99 [0.99–0.99])—but shows limited transfer on institution-specific HOSPITAL (0.02 [0.01–0.03]). Bootstrap CIs confirm that low-support categories produce wide intervals: PATIENT has only 27 spans, yielding CIs spanning 30+ percentage points (e.g., AIMI v1: 0.78 [0.61–0.93]). LOCATION is near-zero across all models.

### Transformer Comparison — SHIELD (Span-Level)

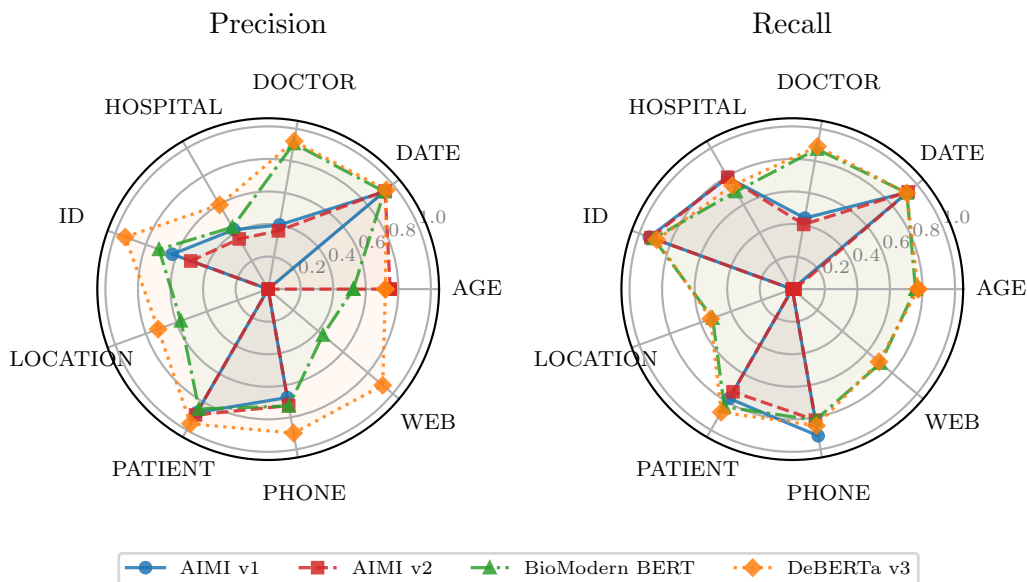


Figure 6: Span-level radar comparison of two distilled student models (DeBERTa v3, BioModern) and two non-student baselines (AIMI v1/v2) on SHIELD. DeBERTa v3 is the best student, achieving the most uniform coverage across all categories. AIMI v1/v2 collapse to zero on AGE, LOCATION, and WEB (absent from their training data), while the distilled students maintain broad coverage.

Together, the cross-dataset results in Figure 8 reveal an asymmetric generalization pattern: SHIELD-trained models (DeBERTa v3, BioModern) generalize well to shared structured categories across both datasets, while domain-specific models (AIMI v1/v2) excel on their home data but do not generalize to categories absent from their training. Institution-specific entities (HOSPITAL, LOCATION) are the hardest to transfer in both directions, whereas universal structured categories (DATE, ID, PHONE) transfer reliably regardless of training data.

### Distillation: Gemini 2.5 Flash vs DeBERTa v3 (Span-Level)

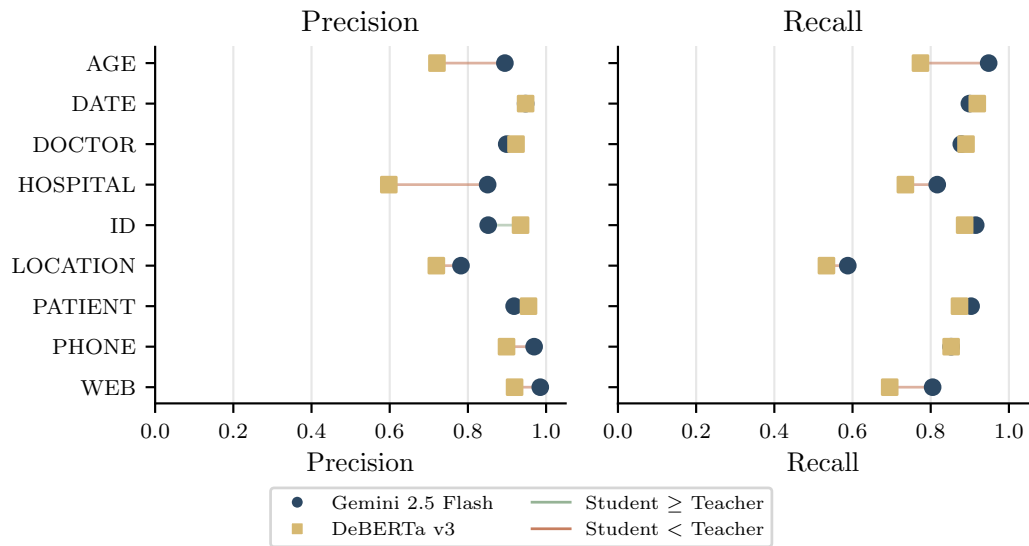


Figure 7: Span-level distillation comparison on SHIELD: Gemini 2.5 Flash (Teacher) vs. DeBERTa v3 (Student). Dumbbell plot showing precision (left) and recall (right) per PHI category. Green connectors indicate student  $\geq$  teacher; red connectors indicate teacher advantage. Full numerical results with bootstrap 95% CIs are provided in Table 2 (Appendix A).

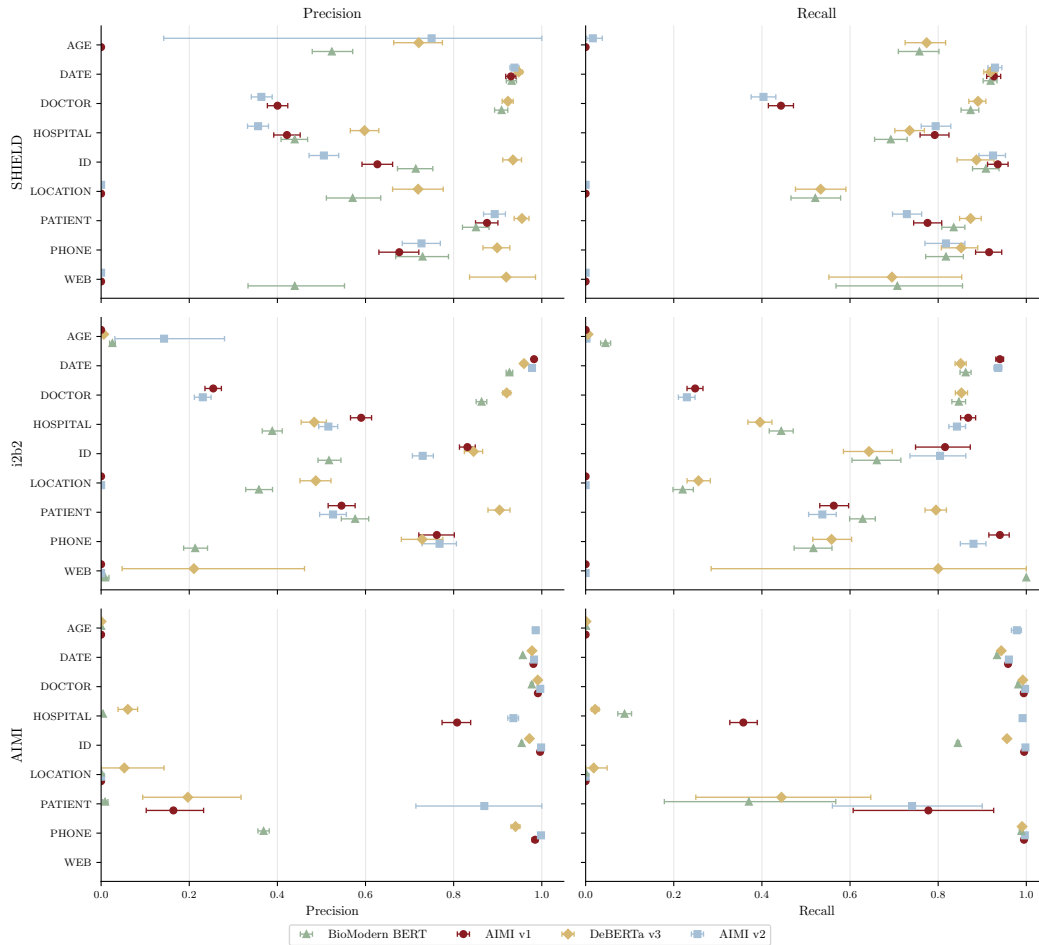


Figure 8: Span-level precision (left) and recall (right) with bootstrap 95% CIs for four transformer models across all three evaluation datasets (SHIELD, i2b2, AIMI). DeBERTa v3 achieves the most balanced coverage on SHIELD, while AIMI v1/v2 show zero recall on categories absent from their training data. Precision patterns reveal complementary trade-offs: AIMI models achieve high precision on their trained categories but produce no predictions (and thus undefined or zero precision) on unseen categories, whereas SHIELD-trained models maintain moderate precision across all categories. Full numerical results are in Tables 3, 4, and 5 (Appendix A).

## 4 Discussion

The results support two key observations for clinical informatics: the value of semantic diversity in benchmarking, and the viability of SLM distillation for secure, enterprise-scale de-identification.

**Design rationale.** Our pipeline incorporates two deliberate selection stages rather than post-hoc ablations. First, the four-way LLM comparison (Figure 5) served as the teacher selection mechanism: by evaluating Gemini 2.5 Flash, Flash Lite, GPT-OSS 120B, and GPT-OSS 20B on the same gold standard, we identified Gemini 2.5 Flash as the strongest teacher based on its leading recall on high-risk categories. Second, the choice of student architectures—DeBERTa v3 and BioClinical ModernBERT—was informed by Antoun et al. [2025], whose controlled comparison showed DeBERTa v3 offers superior sample efficiency while ModernBERT provides long-context and inference-speed advantages. Further ablation on distillation data volume and multi-teacher ensembling are promising directions for future work.

**Distillation effectiveness.** Paired bootstrap tests (Table 2, Appendix A) identify two significant recall degradations from teacher to student: AGE ( $-0.17$ ,  $p = 0.005$ ) and HOSPITAL ( $-0.08$ ,  $p = 0.005$ ). No category shows a significant improvement. Differences on DATE, DOCTOR, ID, LOCATION, PATIENT, PHONE, and WEB are not statistically significant after Bonferroni correction. Low-support categories (WEB, LOCATION) show wide bootstrap CIs, meaning observed differences cannot be distinguished from sampling noise. This pattern is consistent with the cross-institute generalization findings of Yang et al. [2019], who observed similar performance degradation on institution-specific entities. The precision gap on HOSPITAL (teacher: 0.85 [0.82–0.88] vs. student: 0.60 [0.57–0.63], non-overlapping CIs) suggests that distillation from a generative teacher into a token-classification student loses some contextual reasoning, pointing to targeted error correction [Lee et al., 2025] as a promising direction for future work.

**Cost advantage of distillation.** Our evaluation of four LLMs (Figure 5) reveals that all achieve strong performance on SHIELD, but none solves the problem universally: LOCATION recall remains  $\leq 0.70$  for every LLM, and WEB recall hovers around 0.80. The open-weight GPT-OSS models perform comparably to proprietary Gemini models, suggesting that local LLM deployment is technically feasible, but even the smaller GPT-OSS 20B requires substantial GPU infrastructure. The distillation approach sidesteps this trade-off: the STARR-OMOP warehouse contains approximately 633 billion characters ( $\sim 158$  billion tokens at 4 characters per token) of clinical text. Processing this entire volume through Gemini 2.5 Flash on Vertex AI at Flex/Batch pricing [Google Cloud, 2025] would cost an estimated \$23.7k in input tokens ( $\$0.15$  per 1M tokens  $\times$  158B tokens) plus \$670k in output tokens ( $\$1.25$  per 1M tokens  $\times$  536B estimated output tokens), totaling approximately \$694k (see Appendix E for the full derivation). The output token estimate is a conservative lower bound derived from scaling the structured JSON output of the AIMI v2 de-identification pipeline to the full warehouse; actual costs could be higher depending on output verbosity. By contrast, our distillation approach uses Gemini 2.5 Flash once on  $\sim 13$ k notes at an estimated one-time cost of  $\sim \$10$ , after which the DeBERTa v3 model runs locally at negligible marginal cost—a cost reduction of approximately five orders of magnitude. Notably, Gemini Flash Lite is cheaper than Flash yet outperforms it on DATE and PHONE recall (Figure 5), making it a viable alternative teacher for budget-constrained settings. The GPT-OSS models, being open-weight, can run on-premise, but at 20–120B parameters they still require significant GPU compute—far more than the 184M-parameter DeBERTa v3. Recent work on privacy-preserving local LLMs [Wiest et al., 2025] and LLM-powered de-identification frameworks [Singh et al., 2025] confirms the growing interest in cost-effective alternatives to cloud-dependent pipelines. At enterprise scale, efforts to de-identify billions of notes [Kocaman et al., 2025] and optimize institutional pipelines [Prakash et al., 2025] further validate the economic imperative for efficient local models.

**Domain specificity and benchmark diversity.** The AIMI v1/v2 models’ inability to detect WEB and LOCATION (0.00 across all metrics on SHIELD) and near-zero AGE recall underscores the importance of training data breadth. Cross-dataset evaluation (Tables 4 and 5, Appendix A) further quantifies this asymmetric generalization: SHIELD-trained DeBERTa v3 achieves competitive performance (precision/recall) on universal categories across both i2b2 (DOCTOR: 0.92/0.85, PATIENT: 0.90/0.79) and AIMI (DATE: 0.98/0.94, ID: 0.97/0.96), as visualized in Figure 8, while AIMI models show limited generalization on out-of-distribution categories (LOCATION: 0.00 on i2b2). Institution-specific entities prove hardest to transfer: HOSPITAL recall for DeBERTa v3 drops to 0.40 on i2b2 and 0.02 on AIMI, confirming that hospital-name patterns are highly domain-dependent. The AIMI cross-dataset figures for HOSPITAL and LOCATION should be interpreted with the label mapping caveat in mind (Table 7): AIMI’s VENDOR entities map to unified HOSPITAL and AIMI’s HOSPITAL entities map to unified LOCATION, so these cross-dataset comparisons reflect semantically different entity types, which partly explains the low transfer on both categories. The corpus divergence analysis (FTD and JSD; Figure 4) provides independent quantitative confirmation: SHIELD is distributionally distinct from both i2b2 and AIMI in embedding space and vocabulary, reinforcing its value as a challenging and representative benchmark. Surrogate replacement strategies such as Markov-chain-based approaches [Osborne et al., 2025] offer complementary methods for preserving text utility after de-identification. SHIELD’s distinctiveness reflects genuine differences in clinical content: its diversity sampling captures procedural, nursing, and patient-facing documentation absent from legacy discharge-summary-dominated corpora, requiring de-identification models to handle PHI patterns in operative reports, care plans, and patient instructions.

**The case for note-type-specialized models.** While diverse training data improves coverage across PHI categories, the strong performance of AIMI v1/v2 on their home domain (Table 5, Appendix A; Figure 8: AIMI v2 precision/recall of DOCTOR 1.00/1.00, ID 1.00/1.00, HOSPITAL 0.94/0.99) suggests that for high-volume, semi-structured note types such as radiology and pathology reports, specialized models trained on domain-specific data may outperform general-purpose alternatives. These note types follow relatively predictable templates with consistent PHI placement patterns, which a narrowly trained model can exploit effectively. A practical deployment strategy may therefore combine a broad-coverage model like DeBERTa v3 for heterogeneous clinical notes with specialized models for major semi-structured note types, routing documents by note type to the appropriate model. This hybrid approach could leverage the strengths of both paradigms: diversity-trained models for robustness across the long tail of clinical text, and domain-specific models for maximum accuracy on the most common structured formats.

**Scope.** The primary contributions of this work are the release of the SHIELD dataset and the distilled DeBERTa v3 model, together with a distillation framework for producing locally deployable de-identification SLMs. Accordingly, our evaluation focuses on characterizing LLM teacher performance and the fidelity of teacher-to-student knowledge transfer, rather than providing a comprehensive benchmark of existing de-identification systems. A systematic comparison of established pipelines and software—including rule-based systems (e.g., Philter), prior neural architectures (e.g., NeuroNER), and commercial APIs—is an important direction that is best addressed in a dedicated benchmarking study using SHIELD and other datasets. Instructions for accessing both the dataset and the model are provided at [https://github.com/susom/shield\\_dataset](https://github.com/susom/shield_dataset), and we aim to enable exactly such comparative evaluations by the broader community.

**Limitations.** Several limitations should be acknowledged. First, SHIELD contains only 1,394 notes, which limits statistical power for rare PHI categories. Bootstrap 95% CIs quantify this uncertainty: WEB recall for DeBERTa v3 on SHIELD is 0.70 [0.55–0.85], a 30-percentage-point range reflecting only 82 gold-standard spans, and LOCATION recall is 0.53 [0.48–0.59] (495 spans). By contrast, high-support categories yield tight CIs: DATE recall is 0.92 [0.90–0.93] (3,620 spans). On AIMI, PATIENT (27 spans) produces CIs spanning 30+ percentage points, rendering model comparisons on this category unreliable. Second, all notes originate from a single institution (Stanford Health Care via STARR-OMOP), and multi-site validation is needed to confirm generalizability claims. Third, our distillation uses a single teacher model; ensembling multiple teachers or incorporating targeted error correction [Lee et al., 2025] could improve student accuracy on challenging categories.

## 5 Conclusion

The SHIELD dataset establishes a modern, rigorous standard for clinical de-identification benchmarks, prioritizing geographic, demographic, and semantic diversity over sheer size. Paired with our teacher-student distillation framework, we demonstrate that institutions need not rely on expensive, privacy-restricted cloud APIs or massive local GPU clusters. Our distilled DeBERTa v3 model achieves micro-averaged span-level precision of 0.88 and recall of 0.86 on SHIELD—closely matching its cloud-based Gemini 2.5 Flash teacher—while running entirely on local enterprise hardware. Cross-dataset evaluation on i2b2 and AIMI shows that diversity-trained models generalize well on universal, structured PHI categories (DATE, ID, PHONE) but that institution-specific entities (HOSPITAL, LOCATION) remain resistant to cross-domain transfer regardless of training diversity. Conversely, domain-specific models such as AIMI v1/v2 achieve near-perfect accuracy on their home data but do not generalize to PHI types absent from their training. These findings suggest that optimal enterprise deployment may benefit from a hybrid strategy that pairs broad-coverage models for heterogeneous clinical text with specialized models for high-volume, semi-structured note types. Access instructions for the SHIELD dataset and the distilled DeBERTa v3 model are provided at [https://github.com/susom/shield\\_dataset](https://github.com/susom/shield_dataset) to lower the barrier to safe, scalable clinical text de-identification.

## Acknowledgments and Disclosure of Funding

This research was funded, in part, by the Advanced Research Projects Agency for Health (ARPA-H) under award number AY2AX000024. The views and conclusions contained in this document are

those of the authors and should not be interpreted as representing the official policies, either expressed or implied, of the U.S. Government.

We gratefully acknowledge Professor Sylvia Plevritis, Ph.D. (Stanford University), Principal Investigator of this project, for her support of this work. We also thank Todd Ferris (Deputy Chief Information Officer, Stanford University School of Medicine) and Anthea Buchin (Director of Research Technology Application Solutions, Stanford Healthcare) for their leadership and institutional support of this work. We also thank our colleagues Joe Pallas, Hannah Morgan-Cooper, Farnoosh Sheikhi, Shikha Kothari, and Alvaro Alvarez, all of Stanford Healthcare, for their contributions to the research data infrastructure and engineering work that enabled this project.

## References

- Wissam Antoun, Benoît Sagot, and Djamé Seddah. ModernBERT or DeBERTaV3? Examining architecture and data influence on transformer encoder models performance. In *Proceedings of the 14th International Joint Conference on Natural Language Processing and the 4th Conference of the Asia-Pacific Chapter of the Association for Computational Linguistics (IJCNLP-AAACL 2025)*, 2025. URL <https://aclanthology.org/2025.ijcnlp-long.164/>.
- Negar Arabzadeh and Charles Clarke. Fréchet distance for offline evaluation of information retrieval systems with sparse labels. In *Proceedings of the 18th Conference of the European Chapter of the Association for Computational Linguistics (Volume 1: Long Papers)*, pages 420–431, St. Julian’s, Malta, 2024. Association for Computational Linguistics. URL <https://aclanthology.org/2024.eacl-long.26/>.
- Peter Belcak, Greg Heinrich, Shizhe Diao, Yonggan Fu, Xin Dong, Saurav Muralidharan, Yingyan Celine Lin, and Pavlo Molchanov. Small Language Models are the Future of Agentic AI, June 2025. URL <http://arxiv.org/abs/2506.02153>. arXiv:2506.02153 [cs].
- Alison Callahan, Euan Ashley, Somalee Datta, Priyamvada Desai, Todd A Ferris, Jason A Fries, Michael Halaas, Curtis P Langlotz, Sean Mackey, José D Posada, Michael A Pfeffer, and Nigam H Shah. The stanford medicine data science ecosystem for clinical and translational research. *JAMIA Open*, 6(3):ooad054, 08 2023. ISSN 2574-2531. doi: 10.1093/jamiaopen/ooad054. URL <https://doi.org/10.1093/jamiaopen/ooad054>.
- Pierre J Chambon, Christopher Wu, Jackson M Steinkamp, Jason Adleberg, Tessa S Cook, and Curtis P Langlotz. Automated deidentification of radiology reports combining transformer and “hide in plain sight” rule-based methods. *Journal of the American Medical Informatics Association*, 30(2):318–328, January 2023. ISSN 1067-5027, 1527-974X. doi: 10.1093/jamia/ocac219. URL <https://academic.oup.com/jamia/article/30/2/318/6843283>.
- Min Jin Chong and David Forsyth. Effectively unbiased FID and inception score and where to find them. In *Proceedings of the IEEE/CVF Conference on Computer Vision and Pattern Recognition (CVPR)*, pages 6070–6079, 2020. doi: 10.1109/CVPR42600.2020.00611.
- Woojin Chung and Jeonghoon Kim. Exploiting vocabulary frequency imbalance in language model pre-training, 2025. URL <https://arxiv.org/abs/2508.15390>. NeurIPS 2025.
- Somalee Datta, Jose Posada, Garrick Olson, Wencheng Li, Ciaran O’Reilly, Deepa Balraj, Joseph Mesterhazy, Joseph Pallas, Priyamvada Desai, and Nigam Shah. A new paradigm for accelerating clinical data science at stanford medicine, 2020. URL <https://arxiv.org/abs/2003.10534>.
- D. C. Dowson and B. V. Landau. The Fréchet distance between multivariate normal distributions. *Journal of Multivariate Analysis*, 12(3):450–455, 1982. doi: 10.1016/0047-259X(82)90077-X.
- Hannah Eyre, Qiwei Gan, Mengke Hu, Annie Bowles, Johnathan Stanley, Jianlin Shi, Scott L. DuVall, and Patrick R. Alba. Evaluating Clinical Note Deidentification Tools and Transformer Transferability between Public and Private Data from the US Department of Veterans Affairs, June 2025. URL <https://www.medrxiv.org/content/10.1101/2025.03.21.25323520v2>.
- Google Cloud. Vertex AI — Generative AI Pricing. <https://cloud.google.com/vertex-ai/generative-ai/pricing>, 2025. Gemini 2.5 Flash Flex/Batch pricing: \$0.15 per 1M input tokens, \$1.25 per 1M output tokens. Accessed March 2025.

- Pengcheng He, Jianfeng Gao, and Weizhu Chen. DeBERTaV3: Improving DeBERTa using Electra-style pre-training with gradient-disentangled embedding sharing. arXiv preprint arXiv:2111.09543, 2021.
- Paul M Heider and Stéphane M Meystre. An Extensible Evaluation Framework Applied to Clinical Text Deidentification Natural Language Processing Tools: Multisystem and Multicorpus Study. *Journal of Medical Internet Research*, 26:e55676, May 2024. ISSN 1439-4456. doi: 10.2196/55676. URL <https://pmc.ncbi.nlm.nih.gov/articles/PMC11167315/>.
- Martin Heusel, Hubert Ramsauer, Thomas Unterthiner, Bernhard Nessler, and Sepp Hochreiter. GANs trained by a two time-scale update rule converge to a local Nash equilibrium. In *Advances in Neural Information Processing Systems*, volume 30, 2017.
- Qiao Jin, Won Kim, Qingyu Chen, Donald C. Comeau, Lana Yeganova, W. John Wilbur, and Zhiyong Lu. MedCPT: Contrastive Pre-trained Transformers with large-scale PubMed search logs for zero-shot biomedical information retrieval. *Bioinformatics*, 39(11), 2023. doi: 10.1093/bioinformatics/btad651.
- Aman Kansal, Emma Chen, Boyang Tom Jin, Pranav Rajpurkar, and David A. Kim. MC-MED, multimodal clinical monitoring in the emergency department. *Scientific Data*, 12(1):1094, 2025. doi: 10.1038/s41597-025-05419-5. URL <https://doi.org/10.1038/s41597-025-05419-5>.
- Jakob Nikolas Kather, Dyke Ferber, Isabelle C. Wiest, Stephen Gilbert, and Daniel Truhn. Large language models could make natural language again the universal interface of healthcare. *Nature Medicine*, 30:2708–2710, 2024. doi: 10.1038/s41591-024-03259-5.
- Veysel Kocaman, Hasham Ul Haq, and David Talby. Beyond Accuracy: Automated De-Identification of Large Real-World Clinical Text Datasets, December 2023. URL <http://arxiv.org/abs/2312.08495>. arXiv:2312.08495 [cs].
- Veysel Kocaman, Lindsay Mico, Mustafa Aytug Kaya, Nadaa Taiyab, David Talby, Tae Surh, Yuqing Guo, Vivek Tomer, and Robert Kramer. Automated De-Identification, Consistent Obfuscation, and Regulatory Grade Validation of 2 Billion Patient Notes, September 2025. URL <https://www.researchsquare.com/article/rs-6867162/v1>.
- Aleksandar Kovačević, Bojana Bašaragin, Nikola Milošević, and Goran Nenadić. De-identification of clinical free text using natural language processing: A systematic review of current approaches. *Artificial Intelligence in Medicine*, 151:102845, May 2024. ISSN 09333657. doi: 10.1016/j.artmed.2024.102845. URL <https://linkinghub.elsevier.com/retrieve/pii/S0933365724000873>.
- Zeljko Kraljevic, Anthony Shek, Joshua Au Yeung, Ewart Jonathan Sheldon, Mohammad Al-Agil, Haris Shuaib, Xi Bai, Kawsar Noor, Anoop D. Shah, Richard Dobson, and James Teo. Validating transformers for redaction of text from electronic health records in real-world healthcare, October 2023. URL <http://arxiv.org/abs/2310.04468>. arXiv:2310.04468 [cs].
- Rachel Kuo, Andrew A. S. Soltan, Ciaran O’Hanlon, Alan Hasanic, David A. Clifton, Collins Gary, Dominic Furniss, and David W. Eyre. Benchmarking transformer-based models for medical record deidentification: A single centre, multi-specialty evaluation, May 2025. URL <https://www.medrxiv.org/content/10.1101/2025.05.05.25326979v1>.
- Hee-Jin Lee, Zhen Guo, Luchao Jin, and Morteza Moazami Goudarzi. Targeted Error Correction in Knowledge Distillation: Small Language Models Surpass GPT, November 2025. URL <http://arxiv.org/abs/2511.03005>. arXiv:2511.03005 [cs].
- Haolin Li, Tianjie Dai, Zhe Chen, Siyuan Du, Jiangchao Yao, Ya Zhang, and Yanfeng Wang. RAD: Towards Trustworthy Retrieval-Augmented Multi-modal Clinical Diagnosis, 2025. URL <https://arxiv.org/abs/2509.19980>. NeurIPS 2025.
- Jianhua Lin. Divergence measures based on the Shannon entropy. *IEEE Transactions on Information Theory*, 37(1):145–151, 1991. doi: 10.1109/18.61115.

- Zhengliang Liu, Yue Huang, Xiaowei Yu, Lu Zhang, Zihao Wu, Chao Cao, Haixing Dai, Lin Zhao, Yiwei Li, Peng Shu, Fang Zeng, Lichao Sun, Wei Liu, Dinggang Shen, Quanzheng Li, Tianming Liu, Dajiang Zhu, and Xiang Li. DeID-GPT: Zero-shot Medical Text De-Identification by GPT-4, December 2023. URL <http://arxiv.org/abs/2303.11032>. arXiv:2303.11032 [cs].
- Abdul Moeed, Yang An, Gerhard Hagerer, and Georg Groh. Evaluation metrics for headline generation using deep pre-trained embeddings. In *Proceedings of the Twelfth Language Resources and Evaluation Conference*, pages 1796–1802, Marseille, France, 2020. European Language Resources Association. URL <https://aclanthology.org/2020.lrec-1.222/>.
- Bekelu Negash, Alan Katz, Christine J. Neilson, Moniruzzaman Moni, Marcello Nesca, Alexander Singer, and Jennifer E. Enns. De-identification of Free Text Data containing Personal Health Information: A Scoping Review of Reviews. *International Journal of Population Data Science*, 8(1), December 2023. ISSN 2399-4908. doi: 10.23889/ijpds.v8i1.2153. URL <https://ijpds.org/article/view/2153>.
- OpenAI. GPT-OSS: Open-weight models for reasoning, agentic tasks, and versatile developer use cases. arXiv preprint arXiv:2508.10925, 2025. URL <https://huggingface.co/openai/gpt-oss-120b>. Mixture-of-Experts architecture; GPT-OSS 120B (117B total, 5.1B active parameters) and GPT-OSS 20B (21B total, 3.6B active parameters). Apache 2.0 license.
- John D. Osborne, Andrew Trotter, Tobias O’Leary, Chris Coffee, Micah D. Cochran, Luis Mansilla-Gonzalez, Akhil Nadimpalli, Alex McAnnally, Abdulateef I. Almudaifer, Jeffrey R. Curtis, Salma M. Aly, and Richard E. Kennedy. A Markov Chain Replacement Strategy for Surrogate Identifiers: Minimizing Re-Identification Risk While Preserving Text Reuse. *Electronics*, 14(19):3945, October 2025. ISSN 2079-9292. doi: 10.3390/electronics14193945. URL <https://pmc.ncbi.nlm.nih.gov/articles/PMC12536513/>.
- Eva Prakash, Maayane Attias, Pierre Chambon, Justin Xu, Steven Truong, Jean-Benoit Delbrouck, Tessa Cook, and Curtis Langlotz. Improving the Performance of Radiology Report De-identification with Large-Scale Training and Benchmarking Against Cloud Vendor Methods, November 2025. URL <http://arxiv.org/abs/2511.04079>. arXiv:2511.04079 [cs].
- Praphul Singh, Charlotte Dzialo, Jangwon Kim, Sumana Srivatsa, Irfan Bulu, Sri Gadde, and Krishnaram Kenthapadi. RedactOR: An LLM-Powered Framework for Automatic Clinical Data De-Identification, July 2025. URL <http://arxiv.org/abs/2505.18380>. arXiv:2505.18380 [cs].
- Thomas Sounack, Joshua Davis, Brigitte Durieux, Antoine Chaffin, Tom J. Pollard, Eric Lehman, Alistair E. W. Johnson, Matthew McDermott, Tristan Naumann, and Charlotta Lindvall. BioClinical ModernBERT: A State-of-the-Art Long-Context Encoder for Biomedical and Clinical NLP, June 2025. URL <http://arxiv.org/abs/2506.10896>. arXiv:2506.10896 [cs].
- Amber Stubbs and "Ozlem Uzuner. Annotating longitudinal clinical narratives for de-identification: The 2014 i2b2/uthealth corpus. *Journal of Biomedical Informatics*, 58:S20–S29, 2015. doi: 10.1016/j.jbi.2015.07.020. PMID: 26319540.
- Özlem Uzuner, Yuan Luo, and Peter Szolovits. Evaluating the State-of-the-Art in Automatic De-identification. *Journal of the American Medical Informatics Association*, 14(5):550–563, September 2007. ISSN 1067-5027. doi: 10.1197/jamia.M2444. URL <https://doi.org/10.1197/jamia.M2444>.
- Zuo Wang and Ye Yuan. Jensen-Shannon divergence message-passing for rich-text graph representation learning. arXiv preprint arXiv:2512.20094, 2025. URL <https://arxiv.org/abs/2512.20094>.
- Isabella C. Wiest, Marie-Elisabeth Leßmann, Fabian Wolf, Dyke Ferber, Marko Van Treeck, Jiefu Zhu, Matthias P. Ebert, Christoph Benedikt Westphalen, Martin Wermke, and Jakob Nikolas Kather. Deidentifying Medical Documents with Local, Privacy-Preserving Large Language Models: The LLM-Anonymizer. *NEJM AI*, 2(4):AIdbp2400537, March 2025. doi: 10.1056/AIdbp2400537. URL <https://ai.nejm.org/doi/full/10.1056/AIdbp2400537>.

David P Williamson and David B Shmoys. *The design of approximation algorithms*. Cambridge university press, 2011.

Yuli Wu, Fucheng Liu, Rveyda Yilmaz, Henning Konermann, Peter Walter, and Johannes Stegmaier. A pragmatic note on evaluating generative models with Frchet inception distance for retinal image synthesis. In *Proceedings of Medical Imaging with Deep Learning (MIDL)*, 2026. URL <https://arxiv.org/abs/2502.17160>.

Xi Yang, Tianchen Lyu, Qian Li, Chih-Yin Lee, Jiang Bian, William R. Hogan, and Yonghui Wu. A study of deep learning methods for de-identification of clinical notes in cross-institute settings. *BMC Medical Informatics and Decision Making*, 19(Suppl 5):232, December 2019. ISSN 1472-6947. doi: 10.1186/s12911-019-0935-4. URL <https://pmc.ncbi.nlm.nih.gov/articles/PMC6894104/>.

## A Supplementary Tables and Figures

This appendix contains the full numerical tables and per-dataset radar profiles that complement the main-body figures.

Table 1: Span-level precision (P) and recall (R) per PHI category for four LLMs on SHIELD in zero-shot extraction. Support indicates the number of gold-standard spans per category.

Category	Gemini Flash		Flash Lite		GPT-OSS 120B		GPT-OSS 20B		Support
	P	R	P	R	P	R	P	R	
AGE	0.89	0.95	0.79	0.87	0.87	0.83	0.88	0.82	367
DATE	0.95	0.90	0.99	0.95	0.98	0.94	0.98	0.96	3620
DOCTOR	0.90	0.88	0.95	0.92	0.95	0.87	0.95	0.86	2644
HOSPITAL	0.85	0.82	0.65	0.81	0.70	0.75	0.68	0.71	982
ID	0.85	0.92	0.96	0.88	0.93	0.82	0.93	0.87	742
LOCATION	0.78	0.59	0.83	0.68	0.90	0.61	0.74	0.70	495
PATIENT	0.92	0.90	0.93	0.89	0.92	0.85	0.89	0.83	1044
PHONE	0.97	0.85	0.97	0.95	0.98	0.92	0.97	0.92	521
WEB	0.99	0.80	1.00	0.78	0.98	0.79	0.99	0.82	82

Table 2: Span-level distillation comparison on SHIELD: Gemini 2.5 Flash (Teacher) vs. DeBERTa v3 (Student) with bootstrap 95% CIs (2,000 document-level resamples). Support indicates the number of gold-standard spans per category.

Category	Gemini 2.5 Flash		DeBERTa v3		Support
	P [95% CI]	R [95% CI]	P [95% CI]	R [95% CI]	
AGE	"0.89 [0.86-0.93]"	"0.95 [0.93-0.97]"	"0.72 [0.66-0.77]"	"0.77 [0.73-0.82]"	367
DATE	"0.95 [0.93-0.96]"	"0.90 [0.88-0.91]"	"0.95 [0.94-0.96]"	"0.92 [0.90-0.93]"	3620
DOCTOR	"0.90 [0.88-0.92]"	"0.88 [0.86-0.90]"	"0.92 [0.91-0.94]"	"0.89 [0.87-0.91]"	2644
HOSPITAL	"0.85 [0.82-0.88]"	"0.82 [0.79-0.85]"	"0.60 [0.57-0.63]"	"0.74 [0.70-0.77]"	982
ID	"0.85 [0.82-0.88]"	"0.92 [0.88-0.95]"	"0.93 [0.91-0.95]"	"0.89 [0.84-0.93]"	742
LOCATION	"0.78 [0.73-0.83]"	"0.59 [0.53-0.65]"	"0.72 [0.66-0.78]"	"0.53 [0.48-0.59]"	495
PATIENT	"0.92 [0.89-0.94]"	"0.90 [0.88-0.92]"	"0.95 [0.94-0.97]"	"0.87 [0.85-0.90]"	1044
PHONE	"0.97 [0.95-0.98]"	"0.85 [0.81-0.89]"	"0.90 [0.87-0.93]"	"0.85 [0.81-0.89]"	521
WEB	"0.99 [0.95-1.00]"	"0.80 [0.66-0.93]"	"0.92 [0.84-0.99]"	"0.70 [0.55-0.85]"	82

Table 3: Span-level recall of four transformer models on SHIELD with bootstrap 95% CIs. Categories where AIMI models score 0.00 were not represented in their training data. Recall is reported as the primary safety metric for de-identification.

Category	AIMI v1	AIMI v2	BioModern	DeBERTa v3
AGE	"0.00 [0.00-0.00]"	"0.02 [0.00-0.04]"	"0.76 [0.71-0.80]"	"0.77 [0.73-0.82]"
DATE	"0.93 [0.91-0.94]"	"0.93 [0.91-0.94]"	"0.92 [0.90-0.93]"	"0.92 [0.90-0.93]"
DOCTOR	"0.44 [0.41-0.47]"	"0.40 [0.38-0.43]"	"0.87 [0.85-0.89]"	"0.89 [0.87-0.91]"
HOSPITAL	"0.79 [0.76-0.82]"	"0.79 [0.76-0.83]"	"0.69 [0.66-0.73]"	"0.74 [0.70-0.77]"
ID	"0.94 [0.91-0.96]"	"0.92 [0.89-0.95]"	"0.91 [0.88-0.94]"	"0.89 [0.84-0.93]"
LOCATION	"0.00 [0.00-0.00]"	"0.00 [0.00-0.00]"	"0.52 [0.47-0.58]"	"0.53 [0.48-0.59]"
PATIENT	"0.78 [0.74-0.81]"	"0.73 [0.70-0.76]"	"0.84 [0.81-0.86]"	"0.87 [0.85-0.90]"
PHONE	"0.92 [0.88-0.94]"	"0.82 [0.77-0.86]"	"0.82 [0.77-0.86]"	"0.85 [0.81-0.89]"
WEB	"0.00 [0.00-0.00]"	"0.00 [0.00-0.00]"	"0.71 [0.57-0.86]"	"0.70 [0.55-0.85]"

Table 4: Span-level recall of four transformer models on i2b2 2014 (cross-dataset) with bootstrap 95% CIs. AGE is near-zero across all models due to label-definition mismatch. WEB is excluded (only 5 gold spans).

Category	AIMI v1	AIMI v2	BioModern	DeBERTa v3
AGE	"0.00 [0.00-0.00]"	"0.00 [0.00-0.00]"	"0.05 [0.03-0.06]"	"0.01 [0.00-0.01]"
DATE	"0.94 [0.93-0.95]"	"0.94 [0.93-0.94]"	"0.86 [0.85-0.87]"	"0.85 [0.84-0.86]"
DOCTOR	"0.25 [0.23-0.27]"	"0.23 [0.21-0.25]"	"0.85 [0.83-0.86]"	"0.85 [0.84-0.87]"
HOSPITAL	"0.87 [0.85-0.88]"	"0.84 [0.82-0.86]"	"0.44 [0.42-0.47]"	"0.40 [0.37-0.42]"
ID	"0.82 [0.75-0.87]"	"0.80 [0.74-0.86]"	"0.66 [0.60-0.72]"	"0.64 [0.59-0.70]"
LOCATION	"0.00 [0.00-0.00]"	"0.00 [0.00-0.00]"	"0.22 [0.20-0.24]"	"0.26 [0.23-0.28]"
PATIENT	"0.56 [0.53-0.60]"	"0.54 [0.51-0.57]"	"0.63 [0.60-0.66]"	"0.79 [0.77-0.82]"
PHONE	"0.94 [0.92-0.96]"	"0.88 [0.85-0.91]"	"0.52 [0.47-0.56]"	"0.56 [0.52-0.60]"
WEB	"0.00 [0.00-0.00]"	"0.00 [0.00-0.00]"	"1.00 [1.00-1.00]"	"0.80 [0.28-1.00]"

Table 5: Span-level recall of four transformer models on AIMI (cross-dataset) with bootstrap 95% CIs. WEB is excluded (0 gold spans in AIMI). LOCATION and PATIENT have very low support.

Category	AIMI v1	AIMI v2	BioModern	DeBERTa v3
AGE	"0.00 [0.00-0.00]"	"0.98 [0.97-0.99]"	"0.00 [0.00-0.00]"	"0.00 [0.00-0.00]"
DATE	"0.96 [0.96-0.96]"	"0.96 [0.96-0.96]"	"0.93 [0.93-0.94]"	"0.94 [0.94-0.95]"
DOCTOR	"0.99 [0.99-1.00]"	"1.00 [1.00-1.00]"	"0.98 [0.98-0.98]"	"0.99 [0.99-0.99]"
HOSPITAL	"0.36 [0.33-0.39]"	"0.99 [0.99-1.00]"	"0.09 [0.07-0.10]"	"0.02 [0.01-0.03]"
ID	"1.00 [0.99-1.00]"	"1.00 [1.00-1.00]"	"0.84 [0.84-0.85]"	"0.96 [0.95-0.96]"
LOCATION	"0.00 [0.00-0.00]"	"0.00 [0.00-0.00]"	"0.00 [0.00-0.00]"	"0.02 [0.00-0.05]"
PATIENT	"0.78 [0.61-0.93]"	"0.74 [0.56-0.90]"	"0.37 [0.18-0.57]"	"0.44 [0.25-0.65]"
PHONE	"0.99 [0.99-1.00]"	"1.00 [0.99-1.00]"	"0.99 [0.98-0.99]"	"0.99 [0.99-0.99]"
WEB				

### Transformer Comparison — i2b2 (Span-Level)

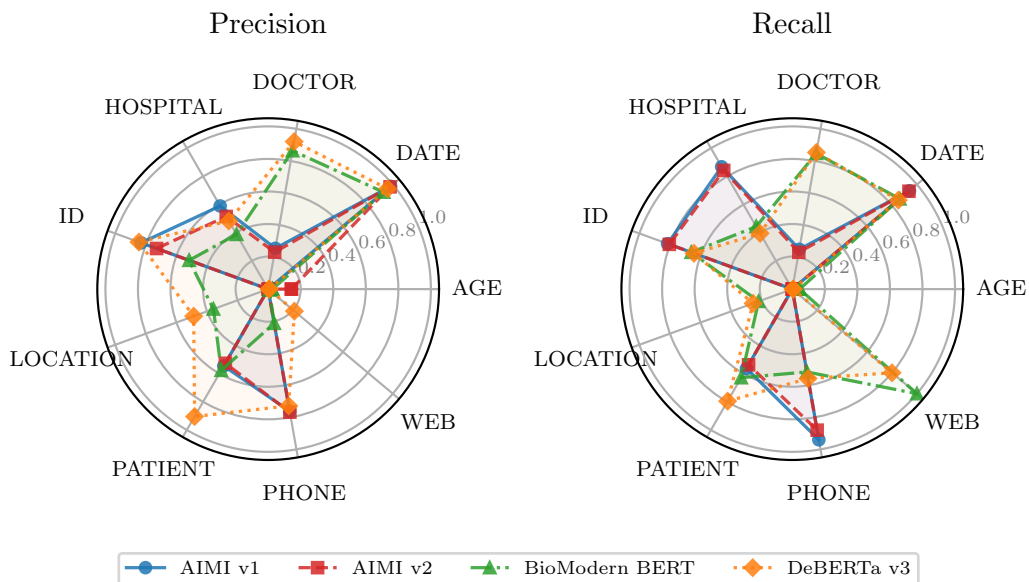


Figure 9: Span-level radar comparison of four transformer models on i2b2 2014 (cross-dataset). DeBERTa v3 achieves the most balanced profile, while AIMI v1/v2 show strong DATE recall but lack coverage on LOCATION.

### Transformer Comparison — AIMI (Span-Level)

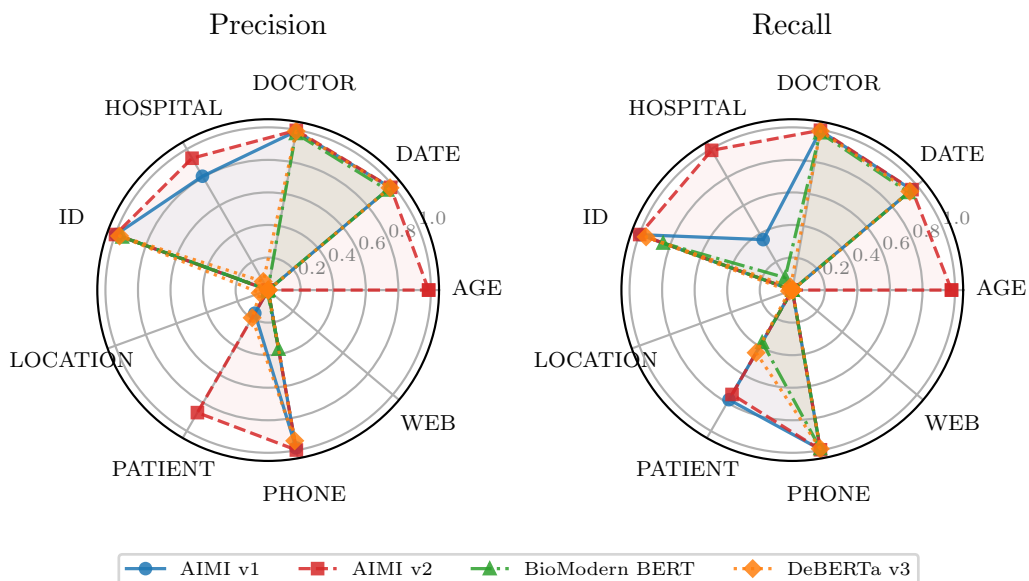


Figure 10: Span-level radar comparison of four transformer models on AIMI (cross-dataset). AIMI v2 dominates on its home data (near-perfect on DOCTOR, ID, HOSPITAL), while DeBERTa v3 and BioModern BERT show competitive recall on universal categories but limited performance on institution-specific HOSPITAL.

## B Unified Label Taxonomy Mappings

To enable cross-dataset evaluation, all gold-standard annotations and model outputs were mapped into a unified canonical label taxonomy consisting of 10 categories: DATE, ID, DOCTOR, PHONE, AGE, HOSPITAL, LOCATION, PATIENT, WEB, and OTHER. Tables 6 and 7 define the complete mappings used in all experiments reported in this paper.

Table 6: i2b2 2014 to unified (SHIELD) label mapping. Multiple fine-grained i2b2 categories are consolidated into broader canonical categories.

i2b2 Label	Unified Label
DATE	DATE
PATIENT	PATIENT
DOCTOR	DOCTOR
MEDICALRECORD	ID
IDNUM	ID
USERNAME	ID
DEVICE	ID
AGE	AGE
HOSPITAL	HOSPITAL
PHONE	PHONE
FAX	PHONE
STREET	LOCATION
CITY	LOCATION
STATE	LOCATION
ZIP	LOCATION
COUNTRY	LOCATION
LOCATION-OTHER	LOCATION
EMAIL	WEB
PROFESSION	OTHER
ORGANIZATION	OTHER

Table 7: AIMI to unified (SHIELD) label mapping. Note that AIMI’s HOSPITAL maps to LOCATION and VENDOR maps to HOSPITAL in the unified taxonomy, reflecting semantic differences in annotation guidelines between datasets.

AIMI Label	Unified Label
DATES	DATE
PATIENT	PATIENT
HCW	DOCTOR
UNIQUE	ID
HOSPITAL	LOCATION
VENDOR	HOSPITAL
PHONE	PHONE
AGE	AGE

## C Token-Level Evaluation Results

Section 3.4 and the main results tables report span-level metrics (see Section 2.5 for the matching criterion). This appendix presents the complementary *token-level* evaluation, where each token is independently classified and scored. Token-level metrics can diverge meaningfully from span-level metrics—for example, a model may correctly tag most tokens within a span but miss the boundary, yielding high token-level recall with lower span-level recall.

All tables below are generated automatically from the evaluation pipeline (see `dataset_models_report.qmd`) and read directly from CSV files to ensure consistency between the report and the paper.

### C.1 LLM Token-Level Performance on SHIELD

Table 8: Token-level precision (P) and recall (R) for four LLMs on SHIELD. Support indicates the number of gold-standard tokens per category.

Category	Gemini Flash		Flash Lite		GPT-OSS 120B		GPT-OSS 20B		Support
	P	R	P	R	P	R	P	R	
AGE	0.90	0.83	0.85	0.94	0.91	0.89	0.92	0.88	1035
DATE	0.98	0.91	0.99	0.96	0.99	0.95	0.99	0.98	17907
DOCTOR	0.94	0.94	0.89	0.94	0.91	0.90	0.91	0.90	9667
HOSPITAL	0.87	0.86	0.68	0.87	0.70	0.83	0.69	0.80	3757
ID	0.90	0.95	0.98	0.90	0.95	0.82	0.95	0.88	3772
LOCATION	0.90	0.58	0.93	0.76	0.97	0.83	0.89	0.87	4674
PATIENT	0.95	0.96	0.95	0.92	0.93	0.90	0.90	0.89	3528
PHONE	0.99	0.93	0.99	0.96	1.00	0.93	0.99	0.93	3473
WEB	1.00	0.95	1.00	0.92	0.99	0.91	0.99	0.95	992

### C.2 Token-Level Distillation Comparison on SHIELD

Table 9: Token-level distillation comparison on SHIELD: Gemini 2.5 Flash (Teacher) vs. DeBERTa v3 (Student).

Category	Gemini 2.5 Flash		DeBERTa v3		Support
	P	R	P	R	
AGE	0.90	0.83	0.82	0.98	1035
DATE	0.98	0.91	0.98	0.99	17907
DOCTOR	0.94	0.94	0.89	0.97	9667
HOSPITAL	0.87	0.86	0.67	0.84	3757
ID	0.90	0.95	0.97	0.93	3772
LOCATION	0.90	0.58	0.87	0.73	4674
PATIENT	0.95	0.96	0.96	0.91	3528
PHONE	0.99	0.93	0.94	0.96	3473
WEB	1.00	0.95	0.97	0.93	992

### C.3 Transformer Token-Level Performance on SHIELD

Table 10: Token-level precision (P) and recall (R) of four transformer models on SHIELD. Categories where AIMI models score 0.00 were not represented in their training data.

Category	AIMI v1		AIMI v2		BioModern		DeBERTa v3		Support
	P	R	P	R	P	R	P	R	
AGE	0.00	0.00	0.75	0.01	0.68	0.97	0.82	0.98	1035
DATE	0.98	0.98	0.97	0.98	0.98	0.99	0.98	0.99	17907
DOCTOR	0.63	0.99	0.60	0.99	0.89	0.95	0.89	0.97	9667
HOSPITAL	0.38	0.63	0.37	0.72	0.58	0.79	0.67	0.84	3757
ID	0.73	0.95	0.60	0.98	0.86	0.93	0.97	0.93	3772
LOCATION	0.00	0.00	0.00	0.00	0.83	0.81	0.87	0.73	4674
PATIENT	0.93	0.85	0.94	0.79	0.91	0.89	0.96	0.91	3528
PHONE	0.81	0.96	0.84	0.84	0.88	0.95	0.94	0.96	3473
WEB	0.00	0.00	0.00	0.00	0.87	0.89	0.97	0.93	992

#### C.4 Transformer Token-Level Performance on i2b2 (Cross-Dataset)

Table 11: Token-level transformer performance on i2b2 2014 (cross-dataset).

Category	AIMI v1		AIMI v2		BioModern		DeBERTa v3		Support
	P	R	P	R	P	R	P	R	
AGE	0.00	0.00	0.14	0.00	0.25	0.90	0.34	0.86	2149
DATE	1.00	0.97	0.99	0.97	0.98	0.95	0.98	0.95	55575
DOCTOR	0.56	0.98	0.53	0.98	0.81	0.93	0.82	0.94	13618
HOSPITAL	0.59	0.96	0.55	0.96	0.63	0.74	0.72	0.73	6460
ID	0.90	0.89	0.83	0.89	0.75	0.72	0.91	0.72	9273
LOCATION	0.00	0.00	0.00	0.00	0.74	0.80	0.70	0.83	4668
PATIENT	0.71	0.96	0.70	0.93	0.77	0.80	0.94	0.82	6253
PHONE	0.85	0.97	0.85	0.91	0.45	0.77	0.80	0.81	2613
WEB	0.00	0.00	0.00	0.00	0.06	1.00	0.35	1.00	46

#### C.5 Transformer Token-Level Performance on AIMI (Cross-Dataset)

Table 12: Token-level transformer performance on AIMI (cross-dataset). WEB is excluded (0 gold tokens in AIMI).

Category	AIMI v1		AIMI v2		BioModern		DeBERTa v3		Support
	P	R	P	R	P	R	P	R	
AGE	0.00	0.00	0.99	0.98	0.01	0.96	0.01	0.97	1033
DATE	0.99	1.00	0.99	1.00	0.99	0.99	0.99	0.99	507934
DOCTOR	0.99	0.99	1.00	1.00	0.97	0.79	0.98	0.76	52137
HOSPITAL	0.82	0.31	0.94	0.99	0.09	0.61	0.43	0.33	6925
ID	1.00	1.00	1.00	1.00	0.99	0.79	0.99	0.97	285974
LOCATION	0.00	0.00	0.00	0.00	0.00	0.00	0.01	0.01	398
PATIENT	0.16	0.82	0.87	0.76	0.01	0.43	0.13	0.42	76
PHONE	0.99	1.00	1.00	1.00	0.37	0.99	0.94	0.99	17464
WEB					0.00	0.00	0.00	0.00	0

## D LLM Extraction Prompt

The following prompt was used for all four LLMs (Gemini 2.5 Flash, Flash Lite, GPT-OSS 120B, GPT-OSS 20B) in the zero-shot extraction evaluation (Figure 5) and for the teacher labeling stage of the distillation pipeline (Section 2.4). The placeholder {clinical\_text} is replaced with the raw clinical note at inference time. The prompt was iteratively refined on a small calibration subset of the SHIELD gold standard (not used for student model training).

*Identify and tag ALL patient-identifiable information and organizational information from clinical notes. Return results as JSON.*

**TOP PRIORITIES (NEVER MISS THESE)**

- DATES:** Scan exhaustively for ALL date formats (MM/DD/YYYY, M/D/YY, M/D, Month DD YYYY, etc.). Include short dates like “4/12” without years. Tag every occurrence separately.
  - EXCLUDE times (10:00AM), temporal words (yesterday), day names (Monday). Example: “2023-03-05T03:43:00-08:00” → “2023-03-05” (exclude T03:43:00-08:00).

2. **COMPLETE ADDRESSES WITH ZIP:** ALWAYS tag addresses in format “Street Address City State ZIP” (note: 2+ spaces between street and city). Example: “1234 MAIN STREET BOSTON MA 02101” is ONE complete entity.
3. **ALL DISTINCT MENTIONS:** Tag each occurrence separately. Do NOT skip any mention because another version exists elsewhere.
4. **EXACT TEXT MATCHING:** Copy text exactly—preserve all case, whitespace, punctuation. Different whitespace = different entity.

#### ENTITY DEFINITIONS

- **PATIENT:** Patient names, relatives, friends, guardians, and any person name that is NOT a healthcare provider. EXCLUDE generic terms (“sister”, “mother”) and titles (Ms./Mr./Mrs., PhD).
- **LOCATION:** ALL address mentions (complete or incomplete). Preserve internal whitespace exactly. EXCLUDE generic facility names (PACU, ICU) without room numbers.
- **DATE:** Any date format. Past, present, future.
- **ID:** MRNs (include hyphens: “1234567-8”), SSNs, account numbers. EXCLUDE generic codes (R07.89), labels without values (“MRN”).
- **AGE:** Complete expressions with units (“72 Y old”, “14 year old”). When units in separate fields (“Age: 14 Units: Years”), tag only number “14”.
- **PHONE:** All formats including pagers. For pagers, tag ONLY number (“12019”), NOT label (“Pgr”).
- **WEB:** Emails, URLs, social media handles, IPs.
- **DOCTOR:** ALL healthcare worker names (providers, nurses, staff, interpreters, coordinators, financial staff). Formal: “Dr. Smith” → “Smith”; “Wilson, Anne Marie, MD” → “Wilson, Anne Marie.”. Informal first names when referring to healthcare workers. EXCLUDE trailing titles; INCLUDE mid-name titles.
- **HOSPITAL:** Organizations, pharmacies, clinics. Room numbers as number only (“3142”, NOT “room 3142”). EXCLUDE generic teams (TT MICU GREEN), generic services (language line).
- **OTHER:** Unique identifying characteristics.

#### KEY RULES

- **Organization + Location Combinations:** Split into HOSPITAL + LOCATION components. Shorthand (org + city/state only): split into separate entities.
- **Multiple Address Formats:** When the same physical location appears in different formats, tag EACH format separately.
- **Exclusions:** Generic facilities (PACU), generic family terms (sister), generic teams (TT CARDIAC ICU), generic services (language line), medical codes (P245).

#### OUTPUT FORMAT

Return valid JSON only. No markdown, explanations, or extra text.

```
{“ENTITY_TYPE”: [{“text”: “exact text”, “confidence”: 0.95}]}
```

Entity types: PATIENT, LOCATION, PHONE, WEB, DATE, ID, HOSPITAL, DOCTOR, AGE, OTHER.

Confidence: 0.00–1.00 (use 0.90–0.99 for clear PHI). No PHI found: return {}. Better to over-tag with lower confidence than miss entities.

*[Two few-shot examples omitted for brevity; available in the released prompt file.]*

```
Clinical Text:
{clinical_text}
```

## E Cost Analysis: LLM Processing vs. Distillation

This appendix provides the detailed cost derivation referenced in the Discussion. All prices are Gemini 2.5 Flash Flex/Batch tier from Google Cloud Vertex AI [Google Cloud, 2025], accessed March 2025. Flash has no long-context surcharge—the price is the same regardless of whether input is  $\leq 200K$  or  $>200K$  tokens.

### E.1 Hypothetical full-warehouse LLM cost

The STARR-OMOP clinical data warehouse contains approximately 633 billion characters of clinical text across all note types. Using a standard rule of thumb of 4 characters per token for clinical English text, this yields an estimated **158 billion input tokens**.

The output token estimate is derived from the structured JSON output of the AIMI v2 de-identification pipeline. Each clinical note produces a JSON object containing identified PHI entities with text spans, entity types, and confidence scores. Scaling the observed per-note JSON output to the full warehouse yields an estimated **536 billion output tokens**. This is a conservative lower-bound estimate; actual output may be larger depending on the density of PHI entities and JSON formatting overhead.

Table 13: Hypothetical cost of processing the entire STARR-OMOP warehouse through Gemini 2.5 Flash (Flex/Batch pricing, March 2025).

Component	Tokens	Price per 1M	Cost
Input (clinical text)	158B	\$0.15	\$23,738
Output (JSON entities)	536B	\$1.25	\$670,000
<b>Total</b>			<b>\$693,738</b>

### E.2 One-time distillation cost

Our distillation pipeline processes only  $\sim 13,000$  notes through Gemini 2.5 Flash. Estimating  $\sim 1,000$  input tokens and  $\sim 500$  output tokens per note:

Table 14: One-time distillation cost using Gemini 2.5 Flash on  $\sim 13k$  notes.

Component	Tokens	Price per 1M	Cost
Input ( $\sim 13k$ notes)	13M	\$0.15	\$1.95
Output (JSON entities)	6.5M	\$1.25	\$8.13
<b>Total</b>			<b>\$10.08</b>

### E.3 Cost comparison

Table 15 summarizes the cost comparison. The distillation approach reduces cloud API costs by approximately five orders of magnitude. After the one-time distillation, the resulting DeBERTa v3 model (184M parameters) runs locally on standard CPU or consumer GPU hardware at negligible marginal cost per note.

Table 15: Cost comparison: full-warehouse LLM processing vs. distillation pipeline. The distillation cost excludes human annotation effort for the 1,394-note SHIELD gold standard and local compute for student model training, which are one-time fixed costs independent of warehouse size.

Approach	Cloud API Cost	Ongoing Marginal Cost
Full warehouse via Gemini 2.5 Flash	\$693,738	\$693,738 per re-run
Distillation (one-time) + local SLM	\$10.08	$\sim \$0$ (local inference)
<b>Reduction factor</b>		$\sim 68,800\times$

#### Assumptions and caveats.

- Token counts use a 4-character-per-token rule of thumb. Actual tokenization depends on the model’s tokenizer (SentencePiece for Gemini) and may vary by  $\pm 20\%$  for clinical text with abbreviations and medical terminology.
- Output token estimates are derived from the structured JSON output of the AIMI v2 pipeline and represent a conservative lower bound.

- Flex/Batch pricing (\$0.15/1M input, \$1.25/1M output) is the lowest available tier; standard pricing (\$0.30 input, \$2.50 output) would double the cost to ~\$1.39M. Priority pricing (\$0.54 input, \$4.50 output) would increase it further to ~\$2.50M.
- The estimate excludes API overhead, network transfer costs, HIPAA-compliant infrastructure, and the operational complexity of processing 158B tokens through cloud APIs while maintaining data governance compliance.
- The distillation cost excludes human annotation labor for the 1,394-note SHIELD gold standard and local compute for student model training, both of which are one-time fixed costs.

## F Corpus Divergence Methods

This appendix provides the full mathematical formulations for the two distributional divergence metrics used in Section 2.3.

### F.1 Fréchet Text Distance (FTD)

Given two corpora  $A$  and  $B$  with document embeddings drawn from  $d$ -dimensional space ( $d = 768$  for MedCPT), we fit multivariate Gaussians  $\mathcal{N}(\boldsymbol{\mu}_A, \boldsymbol{\Sigma}_A)$  and  $\mathcal{N}(\boldsymbol{\mu}_B, \boldsymbol{\Sigma}_B)$  to each corpus. The Fréchet distance [Dowson and Landau, 1982] between these Gaussians is:

$$\text{FTD}(A, B) = \|\boldsymbol{\mu}_A - \boldsymbol{\mu}_B\|^2 + \text{tr}\left(\boldsymbol{\Sigma}_A + \boldsymbol{\Sigma}_B - 2(\boldsymbol{\Sigma}_A\boldsymbol{\Sigma}_B)^{1/2}\right) \quad (1)$$

This decomposes naturally into a *mean shift* component  $\|\boldsymbol{\mu}_A - \boldsymbol{\mu}_B\|^2$  (centroid displacement) and a *covariance divergence* component  $\text{tr}(\boldsymbol{\Sigma}_A + \boldsymbol{\Sigma}_B - 2(\boldsymbol{\Sigma}_A\boldsymbol{\Sigma}_B)^{1/2})$  (differences in spread and shape). The matrix square root is computed via eigendecomposition for numerical stability. This is the text analog of Fréchet Inception Distance (FID) used in image generation evaluation [Heusel et al., 2017]. The application of Fréchet distance to text embeddings was introduced by Moeed et al. [2020], who proposed Fréchet embedding distance for evaluating abstractive summarization using deep pre-trained embeddings, and was later adopted by Arabzadeh and Clarke [2024] for offline evaluation of information retrieval systems under sparse-label conditions.

Bootstrap 95% confidence intervals are computed by subsampling both corpora with replacement 1,000 times, recomputing FTD and its components on each resample, and taking the 2.5th and 97.5th percentiles. We report bootstrap mean estimates as the primary FTD values, since bootstrap resampling with replacement is known to introduce a small upward bias in Fréchet-based distances due to reduced effective rank of resampled covariance matrices [Chong and Forsyth, 2020]; using bootstrap means ensures that reported values fall within their corresponding CIs.

### F.2 Jensen–Shannon Divergence (JSD)

For two corpora with whitespace-tokenized unigram frequency distributions  $P$  and  $Q$  over a shared vocabulary  $\mathcal{V}$ , the JSD [Lin, 1991] is defined as:

$$\text{JSD}(P\|Q) = \frac{1}{2}D_{\text{KL}}(P\|M) + \frac{1}{2}D_{\text{KL}}(Q\|M) \quad (2)$$

where  $M = \frac{1}{2}(P + Q)$  is the average distribution and  $D_{\text{KL}}$  is the Kullback–Leibler divergence:

$$D_{\text{KL}}(P\|M) = \sum_{w \in \mathcal{V}} P(w) \ln \frac{P(w)}{M(w)} \quad (3)$$

JSD is bounded in  $[0, \ln 2]$  and is symmetric. We also compute a *corpus-size-weighted* variant where  $M = \pi_A P + \pi_B Q$  with  $\pi_A, \pi_B$  proportional to corpus sizes, which accounts for the large size imbalance between AIMI (46,313 notes) and the other corpora.

Bootstrap 95% CIs are computed via 1,000 document-level resamples: on each iteration, documents are resampled with replacement from each corpus, unigram distributions are recomputed, and JSD is recalculated.

## G Public Release: Statistics and Demographics

This appendix reports descriptive statistics for the SHIELD gold-standard corpus referenced in Section 2.2: PHI category distribution, note-length distribution, patient demographics, and the most common clinical note types. To match the suppression policy of the public release, cells corresponding to fewer than 10 observations are reported as (<10).

Table 16: PHI category distribution across the 9 canonical SHIELD categories.

Category	Count	Percentage	Mean per note
DATE	3,620	34.5%	2.6
DOCTOR	2,644	25.2%	1.9
PATIENT	1,044	9.9%	0.7
HOSPITAL	982	9.4%	0.7
ID	742	7.1%	0.5
PHONE	521	5.0%	0.4
LOCATION	495	4.7%	0.4
AGE	367	3.5%	0.3
WEB	82	0.8%	0.1

Table 17: Note-length distribution (characters and words per note).

Metric	Min	Q1	Median	Mean	Q3	Max
Characters	430	657	1,010	1,165	1,600	2,518
Words	28	94	145	168	228	437

Table 18: Patient sex distribution (one row per unique patient).

Category	Count	Percentage
FEMALE	518	50.4%
MALE	501	48.8%
No matching concept	(<10)	

Table 19: Patient race distribution (one row per unique patient).

Category	Count	Percentage
No matching concept	310	30.2%
White	301	29.3%
Asian	155	15.1%
Black or African American	135	13.1%
Native Hawaiian or Other Pacific Islander	74	7.2%
American Indian or Alaska Native	52	5.1%

Table 20: Patient ethnicity distribution (one row per unique patient).

Category	Count	Percentage
Not Hispanic or Latino	581	56.6%
Hispanic or Latino	274	26.7%
No matching concept	172	16.7%

Table 21: Patient age distribution (one row per unique patient).

<b>Age band</b>	<b>Count</b>	<b>Percentage</b>
65-79	307	29.9%
50-64	237	23.1%
80+	179	17.4%
35-49	164	16.0%
18-34	111	10.8%
0-17	29	2.8%

Table 22: Top 10 clinical note types by frequency.

<b>Note type</b>	<b>Count</b>	<b>Percentage</b>
letter	45	3.2%
imaging	36	2.6%
procedures	36	2.6%
progress notes	34	2.4%
clinic support note	32	2.3%
patient instructions	32	2.3%
discharge instructions	31	2.2%
telephone encounter	31	2.2%
nursing note	29	2.1%
consults	27	1.9%